Macromolecules

Volume 41, Number 13 July 8, 2008

Review

Recent Developments in Monte Carlo Simulations of Lattice Models for Polymer Systems

K. Binder* and W. Paul

Institut für Physik, Johannes Gutenberg-Universität, Staudinger Weg 7, D-55099 Mainz, Germany

Received December 21, 2007; Revised Manuscript Received March 18, 2008

ABSTRACT: A brief review is given of methodological advances made during the past decade with the Monte Carlo sampling of equilibrium properties of simple lattice models of polymer systems, and representative applications of these new algorithms are summarized. These algorithms include Wang−Landau (WL) sampling, the pruned-enriched Rosenbluth method (PERM), and topology violating dynamic Monte Carlo algorithms such as combinations of local moves, slithering snake moves, and "double bridging" moves for the bond fluctuation model. The applications mentioned concern phase-transition-like phenomena of single chains (collapse and crystallization in bad solvents; interplay of collapse and adsorption; escape of chains from confining tubes; microphase separation in binary bottle brushes) and nontrivial correlation effects in dense systems of many chains (intramolecular long-range correlations in melts; fluctuation effects of micelles in homopolymer−block copolymer blends.) While all these examples refer to work on lattice models, these algorithms are useful for off-lattice models as well. Open problems and directions for future work are briefly addressed.

Introduction

For many decades the statistical mechanics of flexible macromolecules has provided challenging problems, some of which are still not fully understood today. For instance, the standard description of the configuration of a very long polymer chain (consisting of N effective subunits, which we shall call "monomers") is a self-avoiding random walk (swollen coil) in dilute solution under good solvent conditions, i.e., the gyration radius scales as[1–6] $R_g \propto N^{\nu}$, with[7–10] $\nu \approx 0.587$ in $d = 3$ dimensions and $\nu = 3/4$ in $d = 2$ dimensions,[10] while R_g becomes smaller when the solvent quality is reduced (e.g., by lowering the temperature T). Thus, at the Theta-temperature $T = \Theta$ the chain conformations become (almost) that of an "ideal" (i.e., Gaussian or simple random-walk-like) chain,[1–6] $R_g \propto N^{1/2}$, apart from logarithmic corrections,[5,11,12] while for $T < \Theta$ a collapsed state of the chain is predicted, i.e., $R_g \propto (1 - T/\Theta)^{-1/3} N^{1/3}$.[1–6,13] However, recently it was suggested, based on evidence[14–17] from Monte Carlo simulations, that this description is not complete, since an alternative scenario exists, where the above continuous transition is replaced by a discontinuous one, where solvent quality reduction causes a first-order-like transition from the (slightly) swollen coil to a dense crystalline state of high density.

Similarly, another "cornerstone of polymer physics" has been the so-called "Flory ideality hypothesis",[1,2,18–20] which states that flexible polymer chains in three-dimensional dense melts correspond to "ideal" random walks on length scales much larger than the monomer diameter. The justification for this hypothesis, namely that intrachain and interchain excluded volume forces cancel each other exactly when many chains strongly overlap each other, has been widely accepted.[2,6,21,22] However, also this result has recently been called into question.[23–27] There occurs rather a self-similar pattern of nested correlation holes along a chain, leading to distinct deviations from Gaussian behavior. Monte Carlo simulation evidence[25–27] suggests again that these phenomena should be observable in experiments on real macromolecular systems, too.

Progress in both examples mentioned above could only be achieved through the development of new algorithms, which were used for simulations of the well-known bond fluctuation model[28–31] of polymers. Actually, these two ex-

* To whom correspondence should be addressed.

10.1021/ma702843z CCC: $40.75
Published on Web 06/07/2008

Kurt Binder is currently Professor of Theoretical Physics at the Johannes Gutenberg University at Mainz. He received his diploma degree (1967) and his PhD (1969) from the Technical University of Vienna, Austria, and his Habilitation from the Technical University Munich (1973). After postdoctoral stays at IBM Zurich Research Laboratory (1972−1973) and Bell Laboratories, Murray Hill (1974), he was appointed Associate Professor at the University of Saarbrücken (1974−1977); then he became director of an institute at the Solid State Physics Institute of the Research Center Jülich, jointly appointed as Professor at the University of Cologne (1977−1983), from where he moved to his current position. He received numerous distinctions (Max Planck Medal 1993, ISI Highly Cited Researcher 2001, B.J. Alder CECAM Prize 2001, Boltzmann Medal 2007, etc.). His research interests cover many aspects of computational statistical mechanics of condensed matter.

Wolfgang Paul is currently Academic Director and apl. Professor at the Johannes Gutenberg University in Mainz. He received his diploma degree (1986) and his PhD (1989) at this university. After postdoctoral work in Mainz and becoming a staff member of the Physics Institute of Johannes Gutenberg University in 1992, he spent a postdoctoral time at the IBM Almaden Research Center (1993−1994), from where he returned to receive his Habilitation in 1996. His research interests are computational statistical mechanics of polymers and stochastic processes in physics and finance.

amples, which constitute important modifications of the "standard wisdom" on the statistical mechanics of macromolecules, are just two examples out of many where only the application of new algorithms (rather than "brute force" use of very fast computers) allowed substantial progress with the Monte Carlo simulation of polymers. In the present review, we shall outline the main ideas of three selected algorithms developed during the past decade, together with specific applications. Section II will describe the Wang−Landau algorithm[32,33] for the sampling of the energy density of states and will mention applications to the above example of a possible suppression of the fluidlike globular phase of polymer coils at $T < \Theta$ and the interplay between adsorption and collapse of polymer "mushrooms",[34] i.e., chains anchoring with one chain end at a flat substrate surface. Section III will describe the PERM algorithm,[35–39] a recent generalization of the well-known Rosenbluth−Rosenbluth inversely restricted sampling.[40] Application examples will include crossover scaling of very long confined chains[41] and the "escape transition" from confining stripes of finite length[42] and problems relating to the structure of so-called "bottle brush" polymers.[43–45] Section IV then briefly reviews how a combination of local moves with nonlocal ones allows a speed-up of dynamic Monte Carlo sampling by many orders of magnitude,[27] allowing the study of the deviations from Flory's ideality hypothesis, alluded to above. Finally, section V contains an outlook on a few further problems requiring unconventional algorithms (such as moves where homopolymers and block copolymers in a mixture are exchanged, in a study of micelle formation[46]), and section VI discusses open problems as well as possible directions that should be addressed in future work.

We emphasize that this paper is not intended as a review of all the recent important work dealing with Monte Carlo simulations of polymers: such a review would fill a whole book. Thus, we have restricted the scope of the present paper to simple lattice models of (synthetic) polymers, and only static equilibrium properties are considered. Even within this restricted scope we have not attempted to give a complete survey of all the literature, but rather emphasize new methods that are not yet described in the standard textbooks on polymer simulation and describe how the application of such new methods can help to clarify basic problems of theoretical polymer science by reviewing some representative examples.

The Wang−Landau Algorithm and Its Application to Single-Chain Transitions

How To Sample the Energy Density of States. According to the canonical ensemble of statistical mechanics, averages of an observable $A(\vec{X})$ have to be obtained as ($\vec{X}$ stands for a state in the conformation space of the system).

$$\langle A\rangle_T = Z^{-1}\sum_{\vec{X}} \exp[-\mathbf{H}(\vec{X})/k_B T]A(\vec{X}) \tag{1}$$

where T is the absolute temperature, k_B is Boltzmann's constant, $\mathbf{H}(\vec{X})$ the Hamiltonian of the system, and Z the partition function

$$Z = \sum_{\vec{X}} \exp[-H(\vec{X})/k_B T] = \sum_n g(E_n)\exp[-E_n/k_B T] \tag{2}$$

Note that we here have assumed that the phase space $\{\vec{X}\}$ of the model is a set of discrete states (as it is true for lattice models of polymers), but this formalism can easily be generalized to the continuum case, of course. Since each discrete state $\vec{X}$ will yield a corresponding energy $E_n = \mathbf{H}(\vec{X})$, it is clearly possible to transform from the sum over the high-dimensional phase space $\vec{X}$ to the one-dimensional space of energy states $\{E_n\}$, and this transformation done in eq 2 defines the energy density of states, $g(E_n)$. Monte Carlo sampling now amounts to an approximate evaluation of $\langle A\rangle_T$, by replacing the sum over all states $\{\vec{X}\}$ by a sum over a statistical sample of $\mathbf{M}$ states.[31,47,48] If these states $\vec{X}_\nu$ are chosen completely at random, one arrives at the "simple sampling" Monte Carlo method, leading to averages defined as ("ss" stands for "simple sampling")

$$\overline{A}_{ss} = \sum_{\nu=1}^{\mathbf{M}} A(\vec{x}_\nu)\exp[-\mathbf{H}(\vec{X}_\nu)/k_B T]/\sum_{\nu=1}^{\mathbf{M}} \exp[-H(\vec{X}_\nu)/k_B T] \tag{3}$$

While this method (and its ramifications, such as enrichment techniques[49–51]) has yielded useful results for various problems involving single not too long self-avoiding walks,[49,52] it clearly fails for problems involving many polymer chains as well as

for problems involving single but very long chains, however, because it turns out to be impossible to generate enough states in the regions of phase space where the statistical weight $\rho_\nu = \exp[-\mathbf{H}(\vec{X}_\nu)/k_BT]/Z$ is sufficiently large. This problem is rectified by the "importance sampling method" of Metropolis et al.:[47–49,53] phase space points are not sampled uniformly, but preferentially from the "important region" of phase space. That is, one chooses states $\vec{X}_\nu$ with a probability proportional to their weight ρ_ν in thermal equilibrium, such that ("is" stands for "importance sampling")

$$\bar{A}_{is} = \sum_{\nu=1}^{\mathbf{M}} A(\vec{X}_\nu)/\mathbf{M} \tag{4}$$

This is achieved by constructing the states $\vec{X}_\nu$ according to a Markov process $\vec{X}_\nu \rightarrow \vec{X}_{\nu+1} \rightarrow \vec{X}_{\nu+2} \rightarrow ...$, where transitions $\vec{X}_\nu \rightarrow \vec{X}_{\nu+1}$ are carried out such that the transition probability $W(\vec{X} \rightarrow \vec{X}')$ satisfies the detailed balance principle[47–49,53]

$$W(\vec{X} \rightarrow \vec{X}') \exp[-\mathbf{H}(\vec{X})/k_BT] = W(\vec{X}' \rightarrow \vec{X}) \exp[-\mathbf{H}(\vec{X}')/k_BT] \tag{5}$$

Still there is an enormous freedom what the choice $\vec{X} \rightarrow \vec{X}'$ means in practice: for the bond fluctuation model of polymers[28–31] such a move $\vec{X} \rightarrow \vec{X}'$ may entail a local small displacement of a monomer[28–31] or a clever chosen combination of local and nonlocal moves of a chain.[27] In section IV, we shall return to this thought and will show that via a good choice of moves indeed substantial progress can be made.

However, here we rather emphasize a disadvantage of importance sampling that becomes evident when we compare eq 4 with eqs 2 and 3: obviously, all information on the partition function and hence also the free energy $F(T) = -k_BT \ln Z$ of the system has been lost. This is very unfortunate in particular when one wishes to study phase transitions, since at the phase transition of systems in statistical mechanics the free energies of the phases involved in the transition become equal. In addition, the knowledge of F is also required if one wishes to estimate the entropy S, using the relation

$$S(T) = [U(T) - F(T)]/T, \quad U(T) = \langle H \rangle_T \tag{6}$$

For many problems knowledge of the entropy is of great interest.

The advances in simulation methodology discussed in this section and in the following section address this issue, devising methods to estimate the partition function Z and hence also both $F(T)$ and $S(T)$. While the strategy of the PERM algorithm[35,36] is to modify eq 3, choosing state $\vec{X}_\nu$ with weights w_ν, biasing the recursive construction of states such that the weights w_ν turn out to be as large as possible ("bs" stands for "biased sampling").

$$\bar{A}_{bs} = \sum_{\nu=1}^{\mathbf{M}} \{A(\vec{X}_\nu) \exp[-\mathbf{H}(\vec{X}_\nu)/k_BT]/w_\nu\}/Z_{bs} \tag{7a}$$

$$Z_{bs} = \sum_{\nu=1}^{\mathbf{M}} \{\exp[-\mathbf{H}(\vec{X}_\nu)/k_BT]/w_\nu\} \tag{7b}$$

the strategy of the WL method is to devise a recursive algorithm to directly estimate $g(E)$ in eq 2.

The WL method was originally suggested in refs 32 and 33 and applied to spin models on the lattice. It was quickly taken up by other groups and extended to continuum models[54] with applications, e.g., to Lennard-Jones fluids[55–58] and proteins,[59–61] and improvements for the convergence of the method were suggested.[56,62–64] Relations with other flat histogram methods like transition matrix sampling[65] were realized, and the method was generalized to the sampling of the canonical partition function[66] or flat order parameter distributions.[67,68] It has recently also been combined with the PERM algorithm.[69] We base our description here on the original formulation of the method. One still uses importance sampling, but instead of the standard acceptance criterion[47–49,53] for a change of state from "old" to "new"

$$\text{prob}(\text{old} \rightarrow \text{new}) = \text{Min}\{1,\ \exp[-\mathbf{H}(\vec{X}_{old})/k_BT]/\exp[-\mathbf{H}(\vec{X}_{new})/k_BT]\} \tag{8}$$

that satisfies eq 5 one chooses now

$$\text{prob}(\text{old} \rightarrow \text{new}) = \text{Min}\{1, g(E(\vec{X}_{old}))/g(E(\vec{X}_{new}))\} \tag{9}$$

If the density of states of a model is known, this acceptance criterion for a move generates a random walk through configuration space if one uses a set of model specific (ergodic) Monte Carlo moves. When one then records the number of configurations $H(E)$ visited for given energy values E, one should obtain a flat histogram.

Of course, $g(E)$ is a priori unknown, but one can base on eq 9 an iterative procedure to determine the density of states. One starts the iteration with the arbitrary choice $g(E) = 1$ for all E and sets $H(E) = 0$ for all E as well. Whenever in the course of the sampling the energy E is encountered, one replaces $g(E)$ by $fg(E)$ and increments $H(E)$ by replacing $H(E)$ by $H(E) + 1$. Typically, the first choice for this modification factor f is $f = e \approx 2.718$. When the monitored histogram of visits $H(E)$ is sufficiently flat (e.g., in practice one may require the number of visits to any state to be at least 80% of the average number of visits over all states), one changes f by taking $f_{new} = \sqrt{f_{old}}$, and the histogram of visits is reset to zero. In the course of the simulation, the detailed balance condition is not fulfilled because the density of states which determines the transition rates is always updated. Only in the late stages of the iteration, when $f \rightarrow 1$, the method approximately fulfills detailed balance. Empirically, the measured density of states converges to the exact one.

This method determines $g(E)$ only up to an undetermined scale factor, which implies that $S(T)$ is only known up to a (T-independent) additive constant. This constant can be eliminated by requesting that $S(T=0) = 0$. Neither the internal energy $U(T)$ nor the specific heat $C(T)$, which then are calculated as

$$U(T) = \langle E \rangle_T = \sum_n E_n g(E_n) \exp(-E_n/k_BT)/\sum_n g(E_n) \exp(-E_n/k_BT) \tag{10}$$

$$C(T) = [\langle E^2 \rangle_T - \langle E \rangle_T^2]/T \tag{11}$$

are affected by this ambiguity, however.

Of course, one wishes to determine other properties of the chains, e.g., the mean-square gyration radius $\langle R_g^2 \rangle_T$. This can be done, writing

$$\begin{aligned}\langle R_g^2 \rangle_T &= \sum_{\vec{X}} R_g^2(\vec{X}) \exp[-\mathbf{H}(\vec{X})/k_BT]/Z(T) \\ &= \frac{1}{Z(T)} \sum_n g(E_n) \left\{ \frac{1}{g(E_n)} \sum_{\vec{X} \in E_n} R_g^2(\vec{X}) \right\} \exp(-E_n/k_BT) \\ &= \frac{1}{Z(T)} \sum_n g(E_n) \langle R_g^2 \rangle_{E_n} \exp(-E_n/k_BT)\end{aligned} \tag{12}$$

In terms of the generated histogram in the final state of the iteration, this microcanonical average is estimated as

$$\langle R_g^2\rangle_E = \frac{1}{g(E)}\sum_{\vec{X}\in E} R_g^2(\vec{X}) \approx \overline{R_{g,E}^2} = \frac{1}{H(E)}\sum_{\vec{X}\in E} R_g^2(\vec{X}) \quad (13)$$

Note that the sums over $\vec{X}$ in the second line of eq 12 and in eq 13 only run over configurations that belong to the fixed energy E_n (or E, respectively).

Applications: The Phase Diagram of a Single Polymer Chain in the Bulk and at an Attractive Wall. As a first application example, we discuss the bond fluctuation model in a dilute solution of variable solvent quality.[14–17] In this model, monomers are represented as unit cubes on the simple cubic lattice, connected by bonds that can vary in length and direction. The shortest bond length compatible with excluded volume between the monomers is $b = 2$, and the largest allowed bond length of the model is $b = \sqrt{10}$ (measuring all lengths in units of the lattice spacing). The set of allowed bond vectors is generated by the basis vectors (2,0,0), (2,1,0), (2,1,1,), (2,2,1), (3,0,0), and (3,1,0), applying all symmetry operations of the simple cubic lattice. The chains are flexible, and an attractive interaction of the square well type applies, with strength ε and range λ (two choices, $\lambda_1 = \sqrt{6}$ and $\lambda_2 = \sqrt{10}$, will be considered). We now choose units such that $\varepsilon = 1$ and $k_B = 1$. The energy eigenstates E_n in eqs 2, 10, and 12 then simply are given as $E_n = -n_b\varepsilon$, n_b counting the number of pairs within the range λ. The Wang−Landau algorithm allowed to study the specific heat and the mean-square gyration radius over the full temperature range (using a mixture of random hopping moves, "slithering snake" moves, and "pivot moves",[31,49] for chain lengths N in the range from $N = 32$ to $N = 512$.[14–17]

An analysis of these data showed that two (rounded) transitions can be identified: a coil−globule transition characterized by a peak in the specific heat at $T_\Theta(N)$ and a crystallization transition (first observed in ref 70) at $T_{crys}(N)$. Of course, sharp transitions are only to be expected in the limit $N \to \infty$, and so the extrapolation of these (pseudo-) transition temperatures to the thermodynamic limit needs to be considered. For the coil−globule transition, one can infer from the presumed tricritical nature[2,3,5,11,12] of the Θ point that the leading correction should scale like $N^{-1/2}$, and hence the data were fitted to the following formula for the shift of this transition

$$T_\Theta(N) = \Theta - a_1 N^{-1/2} \quad (14)$$

In contrast, for the transition from the liquid globule to the crystal, one can expect the shift to be determined by the relative importance of the surface free energy of the finite system, leading to

$$T_{crys}(N) = T_{crys}(\infty) - b_1 N^{-1/3} \quad (15)$$

Figure 1 shows corresponding extrapolations. For the case of the larger interaction range of the effective attraction between the monomers, $\lambda_2 = \sqrt{10}$, the behavior found here is just the expected one: The coil−globule transition occurs for $\Theta = 4.01 \pm 0.02$, while crystallization occurs for $T_{crys} = 3.20 \pm 0.02$. At this point we mention that the problem of understanding the precise structure of such "solids" formed from a single very long polymer chain is very subtle, and our model (based on an underlying simple cubic lattice) clearly is very remote from the actual crystallization phenomena in real polymers[22,71] which relate to the "packing" of monomers that need to be described by a chemically realistic model in continuum space. The structure found in our model is not a simple cubic arrangement of our effective monomers, but rather one finds a layered sequence ACBC, each layer being a modified hexagonal-like packing that fits on the simple cubic lattice, where the subsequent double layers AC and BC are turned with respect to each other by 90°.[14,15,72] We also emphasize that the characterization of the crystalline phase of single polymer chains may be practically rather unimportant because typically the crystallization will be kinetically hindered, and rather a glassy freezing of the (supercooled) globule may occur, analogous to the glass transition of polymer melts in the bulk.[22,73,74]

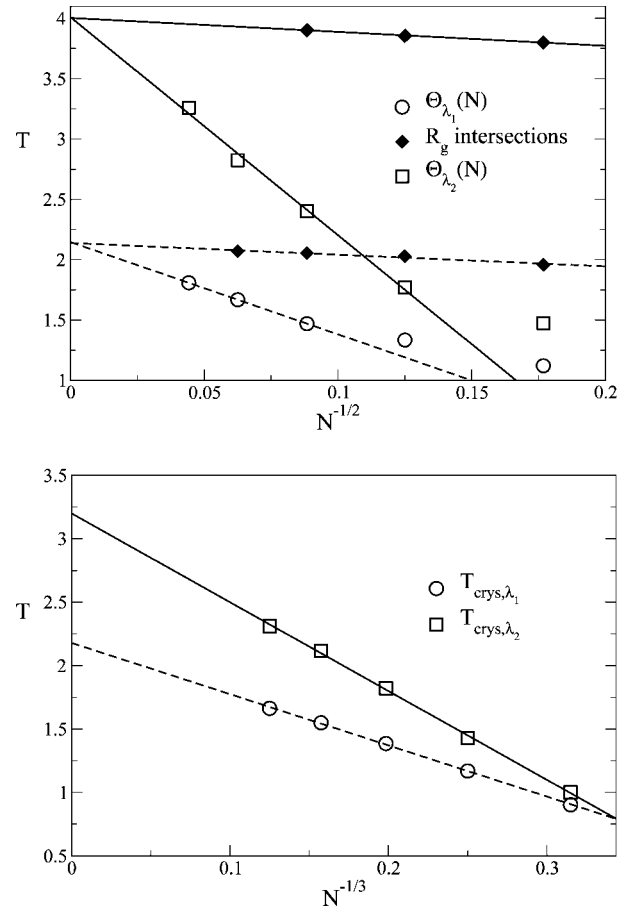

Figure 1. Extrapolation of the location of the coil−globule transition (top) and the crystallization transition (bottom) located by the higher (top) or lower (bottom) peak position found in the specific heat vs temperature curves. Open circles refer to λ_1 and squares to λ_2. The diamonds in the top part refer to intersection points of pairs of curves $\langle R_g^2(T)\rangle/N$ vs T for N and $2N$, respectively (since $\langle R_g^2\rangle \propto N^{2\nu}$ for $T > \Theta$, $\langle R_g^2\rangle \propto N^{2/3}$ for $T < \Theta$ while, roughly, $\langle R_g^2\rangle \propto N$ for $T = \Theta$, such intersection points should also converge toward Θ as $N \to \infty$ and, in fact, yield estimates nicely compatible with the extrapolation of the specific heat peaks, as the figure shows). Reproduced with permission from ref 17. Copyright 2007 American Institute of Physics.

A very interesting and rather unexpected behavior occurs for the second choice with the shorter interaction range, $\lambda_1 = \sqrt{6}$, however: Figure 1 implies that $T_{crys}^{(\infty)} = 2.18 \pm 0.01$ and $\Theta = 2.14 \pm 0.04$, i.e., Θ and T_{crys} coincide, within statistical errors! So, unlike the case with $\lambda_2 = \sqrt{10}$, where the liquid globular state exists for an extended temperature range, $3.2 \le T \le 4.0$ or thereabout, we do not observe a liquid globule any longer, for $N \to \infty$ and an interaction range $\lambda_1 = \sqrt{6}$. This conclusion is corroborated by a study of the density of the liquid globule that coexists with the crystal at $T = T_{crys}(N)$ for finite N: while for $\lambda_2 = \sqrt{10}$ this density converges to a nonzero finite value, $\rho_{liq}^{coex}(N) \approx 0.66 + 0.4N^{-0.153}$ providing a good fit to the data,[17] for λ_1 one rather finds[15–17,72] $\rho_{liq}^{coex}(N) \propto N^{-0.153}$, implying that for $N \to \infty$ a globular phase (which must have $\rho_{liq}^{coex} > 0$) no longer exists. Note also that the quoted value of the exponent (0.153) in these relations is purely empirical and lacks any

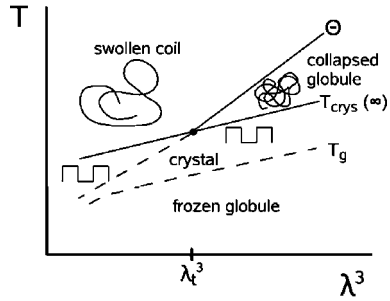

Figure 2. Schematic phase diagram of a single chain in the limit $N \rightarrow \infty$ (and infinite dilution) in the plane of variables temperature T and interaction volume λ^3 of the attractive interaction (note that transition temperatures should increase linearly with λ^3 for ε = constant at large λ; therefore, all transition curves have been drawn as straight lines). Phases indicated are the swollen coil ($T > \Theta$), collapsed globule $\{T_{crys}(\infty) \leq T \leq \Theta\}$, and the crystal $\{T \leq T_{crys}(\infty)\}$. Below the glass transition temperature T_g the collapsed globule may exist as a frozen metastable state (apart from higher density, its structure is qualitatively similar to the liquid state of the collapsed globule). At $\lambda = \lambda_t$, the lines $\Theta(\lambda)$ and $T_{crys}(\lambda)$ meet, and for $\lambda < \lambda_t$ the collapsed globule may only exist as a metastable state {also the swollen coil may then exist for $T < T_{crys}(\infty)$ but above the metastable continuation of $\Theta(\lambda)$ as a metastable state}.

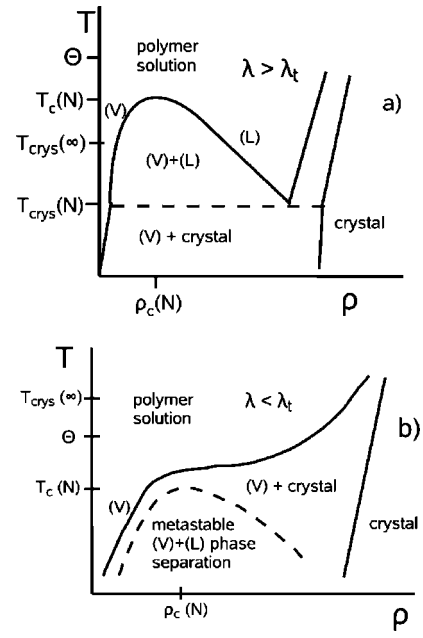

Figure 3. (a) Sketch of the phase diagram of a polymer solution with $\lambda > \lambda_t$, which has a upper critical solution temperature $T_c(N)$; for $T < T_c(N)$ phase separation occurs into a dilute solution (analogous to the vapor (V) of a molecular system) and a concentrated solution (analogous to the liquid (L)). The critical volume fraction $\rho_c(N)$ corresponds to the critical density of a molecular system; note, however, that $\rho_c(N) \rightarrow 0$ and $T_c(N) \rightarrow \Theta$ as $N \rightarrow \infty$. Here it is also assumed that the polymer can crystallize, and complications like glassy freezing or appearance of semicrystalline states consisting of crystalline lamellae and amorphous regions in between are disregarded. (b) Same as (a) for $\lambda < \lambda_t$ and sufficiently large chain length N. Now the upper critical solution temperature $T_c(N)$ exists, if at all, only in the metastable undercooled polymer solution underneath the solution−crystal coexistence curve, and is shown by a broken curve. Here Θ is the infinite chain length limit of the metastable critical point.

theoretical explanation so far. So the qualitative phase diagram of a single *flexible* chain in the limit $N \rightarrow \infty$ should look like speculatively drawn in Figure 2, taking temperature and interaction volume λ^3 as parameters.

A very interesting question then is to ask what this implies for the phase diagram of a polymer solution with finite chain length N, when the volume fraction ρ of the monomers in the solution is varied. The standard phase diagram, applicable for $\lambda > \lambda_t$, is shown in Figure 3a; it has the same topology as the phase diagram of a simple molecular system, when ρ is interpreted as the density in the system, and the dilute solution corresponds to the vapor phase. If $\lambda < \lambda_t$, however, rather the triple line at $T_{crys}(N)$, where dilute solution (or vapor (V)), concentrated solution (or liquid (L)), and crystal can coexist, has disappeared, and a phase diagram having the "swan neck" topology remains, where (in equilibrium, disregarding any glassy states and metastable phase segregation in the polymer solution) a more or less dilute solution and the crystal coexist.

The phase diagrams in Figure 3 actually are very much reminiscent of phase diagrams of colloid−polymer mixtures, where the polymers induce a short-range square-well-type attractive depletion interaction between the colloidal particles.[75–77] Denoting the radius of the colloidal particles as σ, it is useful to define a scaled width of the square well attraction as $R = \lambda/\sigma - 1$. It was found[75–77] that $R_c = 0.25$ is the critical value separating the two scenarios in Figure 3, for the colloids. It is tempting to carry this consideration over to the present case. If we tentatively put $\sigma = 2$ as the hard-core diameter of the bulky monomers (remember that this is the minimum distance of any pair of monomers in our model), we would estimate that λ_1 corresponds to $R_1 = 0.225$ and λ_2 to $R_2 = 0.58$. It is gratifying that indeed λ_2 is clearly larger than R_c, while λ_1 is slightly smaller than (but very close to) R_c (R_c should correspond to λ_t in Figures 2 and 3, of course).

While it was well-known that increasing chain stiffness may also lead to a similar suppression of gas−liquid type phase separation in polymer solutions as shown in Figure 3b,[4,78–81] and this correlates with a first-order collapse transition of stiff chains[4,78–84] (involving then also local orientational order, toroidal structures, etc.[82–84]), it was an unexpected finding that the theoretical description of the collapse of flexible chains, which does not explicitly exhibit any parameter playing the role of λ_t and hence describes only the continuous behavior found here only for $\lambda > \lambda_t$, still is incomplete. The methodic progress in the Monte Carlo simulation, achieved by the Wang−Landau algorithm,[32,33] was absolutely crucial for allowing a conclusive study of the problem, as shown via the data in Figure 1 and hence to add an interesting facet to our theoretical understanding of polymers. Note that early work trying to estimate the Θ-point for the model with $\lambda = \lambda_1$ produced conflicting evidence[35,85] and could not locate $T_{crys}(N)$. So the availability of efficient algorithms has been clearly necessary for making progress. Clearly, it would be interesting to search for experimental systems which yield the phase diagram of type Figure 3b.

We now turn, only very briefly, to discuss how this picture changes when instead of an unconstrained chain in free space we consider a polymer chain endgrafted to an (attractive) surface. Then a second energy scale ε_w (measuring the energy which is won when a monomer is adjacent to the wall) in addition to ε comes into play, and correspondingly due to the competition between both types of enthalpies and the configurational entropy of the chain, a very complicated behavior may arise.[34,86–95] The understanding of these phenomena is still in its early stages.

If both $\varepsilon = 0$ and $\varepsilon_w = 0$, and the simple random-walk model is considered the only interaction which matters for the structure of the polymer "mushroom"[96] is the entropic repulsion due to the substrate surface (uncrossable for the polymer) to which the chain is grafted. This problem is solved since long ago.[97] However, the problem gets very rich when one considers chains

with excluded volume interactions rather than ideal Gaussian chains.[52,98] The partition function of the mushroom then involves a nontrivial exponent γ_1, $Z_N \propto N^{\gamma_1-1}q^N$, $N \to \infty$, while q is the same (nonuniversal) constant which appears also for the partition function in the bulk.[2,8,98,99] The detailed geometrical structure of mushrooms still is a subject of detailed studies.[100] When now still $\varepsilon = 0$ but $\varepsilon_w > 0$, the possibility of an adsorption transition arises (see e.g. refs 34, 52, 92, 98, 101, and 102). Strongly adsorbed chains take quasi-two-dimensional so-called "pancake"[96] conformations, while the weakly adsorbed chains near the adsorption threshold $\varepsilon_{w,\mathrm{crit}}$ involve several "critical exponents"[52,98] to describe their partition function which are still debated (see e.g. refs 92 and 102).

Introducing now $\varepsilon \neq 0$ the adsorption of the chain competes with its collapse and/or crystallization, and the resulting structures clearly may get strongly changed due to the presence of a constraining surface.[34] So far, a single study of the bond fluctuation model with $\lambda_1 = \sqrt{6}$ has been made, all other work concerns the standard self-avoiding walk model[99] with nearest-neighbor attraction;[86–91,93–95] it is clear that this choice corresponds to a different value of the parameter λ (or R_c, respectively), and since also the possible crystal structures depend on the details of the models, it is hard to judge which aspects of the results for the strongly adsorbed and/or strongly collapsed states are universal. So far, it is clear that one expects "adsorbed-extended (AE)" states when ε_w is large while ε is small, "desorbed extended (DE)" states when both ε_w and ε are small (i.e., ordinary "mushrooms"), while the case of large ε and $\varepsilon_w = 0$ corresponds to collapsed globules or crystals, respectively, which touch the wall only marginally and hence are "called" desorbed collapsed" (DC). States where both ε_w and ε are large may lead to compact two-dimensional coils ("adsorbed compact (AC)"). However, a state resembling a droplet sitting at an incompletely wet surface, where a nonzero contact angle occurs, also has been suggested;[89–92] the parameter region where this "surface attached globule" (SAG) may occur (or related layered crystalline states[34,93]) still is a subject of current discussion.[94] For such a problem, the Wang−Landau[32,33] sampling needs to be extended to a two-variable density of states $g(E_w, E_b)$, where $E_w = -n_w\varepsilon_w$ and $E_b = -n_b\varepsilon$, as above; n_w counts in each configuration the number of monomers which are within the range λ_w of the attraction exerted by the wall. It is clear that an accurate sampling of such a two-dimensional density of states is a much more demanding task, but in view of the many phases and many transitions between them a straightforward study by standard Monte Carlo algorithms[8,31,47–49] hardly would be possible.

Figure 4 shows a preliminary diagram of the states that were found for $N = 64$ for the bond fluctuation model.[34] So far, a conclusive extrapolation toward $N \to \infty$ could be done only in parts of the phase diagram, while large uncertainties about the phase diagram still occur in the region where several of the (rounded) transitions meet; often it then is still impossible to distinguish well-defined peaks in the specific heat, and this is the reason why some of the curves drawn in Figure 4 end somewhere rather than meeting another line: in this way we simply display our incomplete knowledge how such a line will continue.[34] At this point the methodology explained in this section clearly reaches its present limitations.

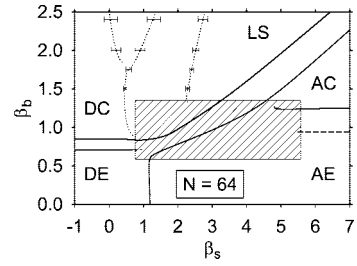

Figure 4. States of a polymer mushroom of length $N = 64$, in the plane of variables of bulk coupling $\beta_b = \varepsilon/k_BT$ and surface coupling $\beta_s = \varepsilon_w/k_BT$. Depending on the strength of these energy parameters, different states may occur: standard swollen mushrooms are denoted as "desorbed expanded (DE)", while for large β_b but β_s near zero collapsed mushrooms almost detached from the wall occur ("desorbed collapsed (DC)"). For large β_s but small β_b one encounters two-dimensional swollen configurations ("adsorbed expanded (AE)"); if β_b increases, one encounters two-dimensional collapse toward "adsorbed collapsed (AC)" states. If β_s and β_b are both large and of the same order, "layered states (LS)" occur. The solid lines represent maxima of fluctuations in the number of bulk or surface contacts, while the dashed and dotted lines are estimates from weaker anomalies (shoulders) in these quantities. In the shaded area not all maxima can be identified clearly. Reproduced with permission from ref 34. Copyright 2008 American Institute of Physics.

The Pruned-Enriched Rosenbluth Method (PERM) and Its Application To Study Very Long Chains

As explained in the previous section, WL sampling amounts to a diffusive exploration of the space of energy states (from the ground-state energy $E_{\min}$ to the maximum energy $E_{\max}$ that needs to be considered). Since $E_{\max} - E_{\min} \propto N$, this method clearly becomes impractical when N is very large. An additional difficulty occurs when no energy scale exists in the problem, such as the problem of the "escape transition" of a mushroom confined underneath a disk.[103–112] This transition is purely entropically driven, and if one wishes to characterize it accurately by simulations, very long chains are needed. The latter statement also applies to the study of dimensional crossover problems, such as the $3d - 2d$ crossover of a chain confined between two parallel plates.[113,114]

This class of problems can now be handled by the PERM algorithm, where the use of chains containing of the order of $N = 50\,000$ or even more is current standard.[35,36,41,42,114] The algorithm has also been combined with the WL approach to the so-called flatPERM[69] and applied, e.g., to phase transitions of tethered chains.[94,115,116]

Again we refrain from giving technical details, just emphasizing only the spirit of the approach. The basic idea is the biased chain growth algorithm of Rosenbluth and Rosenbluth.[40] There one constructs a self-avoiding walk configuration of a chain, adding one monomer after the other, but choosing randomly only from those lattice sites for the monomer to be added for which the excluded volume constraint is satisfied, and calculates the weight w_ν (eq 7) of each configuration recursively. In this way one avoids (at least to a large extent) the so-called "attrition problem" of the naive version of simple sampling of self-avoiding walks (eq 3), where due to the excluded volume constraint the probability that a randomly generated configuration on the lattice does not intersect itself decreases exponentially with N, and hence simple sampling is unsuitable to sample states for large N. While the Rosenbluth−Rosenbluth sampling does allow to generate states for very large N, it suffers from the problem that the range over which the weights w_ν vary increases exponentially with N, leading to uncontrollable errors.[49]

This problem is rectified by PERM to a large extent, generating not a single chain step by step but letting a whole population of chains grow in parallel and using a resampling technique ("population control"[35,36]). This means PERM suppresses too large fluctuations in the weights by "pruning"

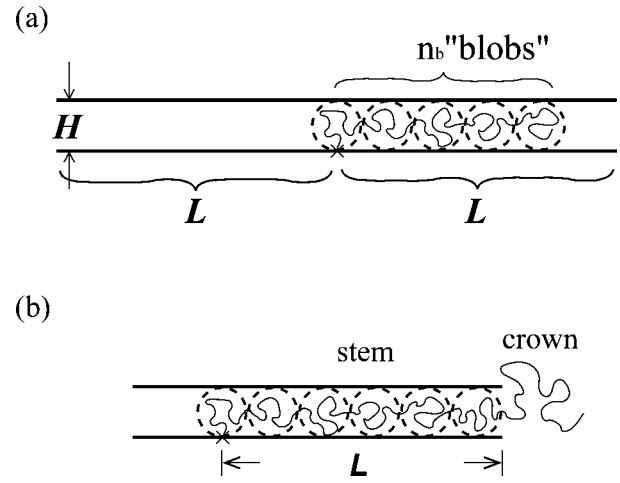

Figure 5. Sketch of a flexible polymer with N monomers grafted in the middle of a strip of length $2L$ and width H, in a blob picture: (a) When the chain is "imprisoned" inside the strip, it forms a sequence of n_B blobs. (b) When the chain length N exceeds the maximum length N^* of a chain in an imprisoned state, the chain partially escapes from the strip and forms an "escaped" state, consisting of a "stem" containing N^* monomers and a "crown" containing $N - N^*$ monomers. Reproduced with permission from ref 42. Copyright 2007 American Institute of Physics.

configurations with too low weight; i.e., those states are thrown out, and on the other hand one enriches the population with copies of high-weight configurations. These copies are made while the chain is growing and continue to grow further independently of each other. This type of algorithm goes under many names ("go with the winners"[35] or "Russian roulette and splitting",[117] "sequential importance sampling with resampling"[118]).

Pruning and enrichment are done by choosing thresholds $W_n^<$ and $W_n^>$ depending on the estimate of the partition sums of chains containing n monomers. If the weight W_n of a chain with n monomers is less than $W_n^<$, the chain is discarded with probability 1/2, while when one keeps it, its weight is doubled. On the other hand, if W_n exceeds $W_n^>$, one produces k identical copies of this configuration, replaces their weight W_n by W_n/k, and uses all these copies as members of the population for the next step, when one adds a monomer to go from chain length n to $n + 1$. Note that this algorithm not only works for athermal chains, Boltzmann factors (depending on the numbers of nearest-neighbor contacts, for instance) are readily included in the recursive calculation of the weights.[35,36,43–45] The algorithm is not only applicable for linear chains but can also be applied to star polymers[37,38] and bottle-brush polymers:[43–45] then all side chains of the bottle brush (or all arms of the star) are grown simultaneously, by adding one monomer to each side chain one after the other, before the growth process of the first side chain continues. We also mention that many variants of this algorithm exist in the literature, and if it is useful, a bias in the chain construction is readily included (but must be taken into account in the computation of the weights W_n, of course). For example, for the bottle-brush simulations a biased growth of the chains preferentially in the direction normally outward away from the (rigid) linear backbone was used.[43–45]

Application of PERM To Study Unconventional Phase Transitions. Our first example deals with a flexible polymer in $d = 2$ dimensions that is grafted with one end in the middle of a strip of length $2L$ and width H (Figure 5). The questions that are asked are the following: for which range of N is the chain imprisoned? And when it escapes, how many monomers N^* remain in the "stem" (Figure 5)?

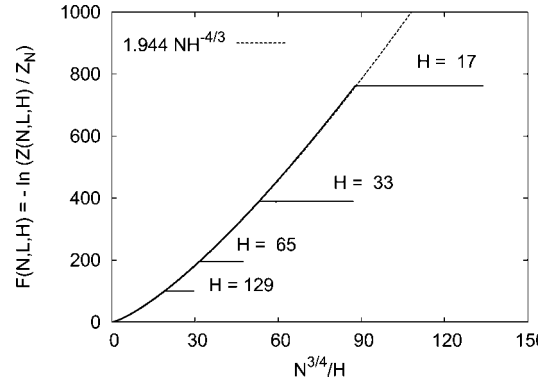

Figure 6. Free energy relative to the free energy of a free chain, $F(N, L, H) = -\ln[Z(N, L, H)/Z_0(N)]$, plotted against $N^{3/4}/H$ for $L = 6400$ and $H = 17$, 33, 65, and 129, for a self-avoiding walk model on the square lattice (lengths are measured in units of the lattice spacing.) The dashed curve is $F_{\text{imp}}(N, L, H) = 1.944NH^{-4/3}$ and gives the best fit to the data. A normalization $k_BT = 1$ is used here. Reproduced with permission from ref 42. Copyright 2007 American Institute of Physics.

Clearly, this problem is a kind of academic "toy problem", but given the possibilities to manipulate biopolymers such as DNA in artificial nanostructures such as arrays of cylindrical tubes, etc.,[119] it probably is an indispensable first step toward more practically useful theoretical exercises.

Let us first sketch the description of the problem in terms of the standard blob picture.[120] We have a "cigar" of n_b blobs of diameter $H = 2r_b$ in the imprisoned case and inside a blob self-avoiding walk statistics holds. So if g monomers belong to a blob, we have $H = ag^{3/4}$, where a is a constant, since $\nu = 3/4$ in $d = 2$ dimensions. Since every monomer of a chain in an imprisoned state must be in a blob, $N = n_b g = n_b(H/a)^{4/3}$, and the end-to-end distance of the cigar then is $R = n_b H = Na(H/a)^{-1/3}$. The free energy excess of the chain in an imprisoned state (in units of k_BT) relative to an unconfined mushroom is simply the number of blobs, $F_{\text{imp}} = n_b = N(H/a)^{-4/3}$. The maximum length N^* of an imprisoned chain is given by the condition that $R = L$, yielding $N^* = (L/a)(H/a)^{1/3}$. Since the free energy of an unconfined mushroom is taken as zero reference point, the "crown" does not contribute to the excess free energy of the escaped chain, which is due to the "stem" alone, $F_{\text{esc}} = N^*(H/a)^{-4/3} = L/H$.

When we increase N at fixed L and H, the blob picture predicts to have a kink in the free energy for $N = N^*$. Now it is clear that the blob picture is somewhat simplified, and for no finite N can a singularity in the free energy or its derivatives be expected. However, a phase transition is possible when we take both $N \to \infty$ and $L \to \infty$ together such that their ratio L/N remains as a convenient control parameter.

Testing this simple description by Monte Carlo simulations using PERM, the power of the algorithm is clearly obvious since free energy differences are readily accessible (Figure 6). One indeed finds results for the free energy branches that are compatible with the blob picture, namely $F_{\text{imp}}(N, L, H) \approx 1.944NH^{-4/3}$ and $F_{\text{esc}} = 2.03L/H$ (describing the horizontal branches in Figure 6). However, the value of the simulation is not only that it can yield prefactors (of order unity, such as the numbers 1.944, 2.03) that are lost in the blob picture; the simulation also gives evidence for more subtle phenomena, that the blob picture fails to describe. According to the blob picture, one would predict that the number of imprisoned monomers N_{imp}, relative to their total number, increase linearly with L/N until the fully imprisoned state ($N_{\text{imp}}/N = 1$) is reached. A more

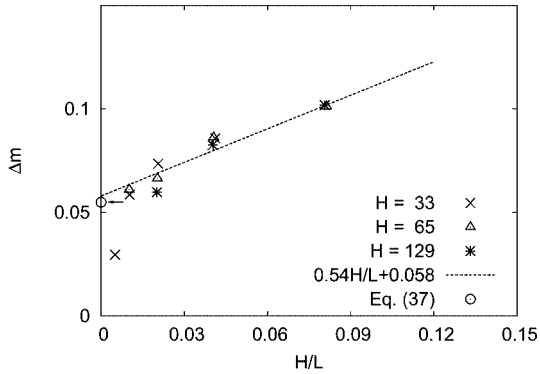

Figure 7. Relative reduction in the number of imprisoned monomers, Δm, plotted against H/L for three choices of H. The dotted straight line is a fit to the data, as indicated in the figure. The open circle gives the theoretical prediction, $\Delta m = 1 - 3/2^{5/3} \approx 0.055$. Reproduced with permission from ref 42. Copyright 2007 American Institute of Physics.

detailed theory[42] implies, however, that the maximum number of imprisoned monomers in escaped states deviates distinctly from N; we have $N_{\mathrm{imp}}^{\mathrm{max}} = N(1 - \Delta m)$ with $\Delta m = 0.055$. The simulations confirm this first-order character of the 2d escape transition in the considered limit (Figure 7).

As a second example of applications of PERM, we mention the problem of binary (AB) bottle-brush polymers. Such polymers are of potential interest as building blocks for various applications, and hence have been studied in various experiments (e.g., refs 121 and 122). It has been suggested that unfavorable interactions between unlike monomers may lead to a "Janus-cylinder" type phase separation in these molecules:[123,124] the molecule has an overall cylindrical shape, but there occurs a planar AB interface containing the cylinder axis, such that the A monomers are preferentially on the one side of the interface and the B monomers on the other side.

This hypothesis was tested by a lattice model,[43,44] the backbone (cylinder axis) of the bottle brush being oriented along the z-axis of the simple cubic lattice, and alternatingly A and B side chains are grafted, with side chain length N and grafting density σ. Taking into account the fact that binary interactions $\varepsilon_{\mathrm{AB}}$, $\varepsilon_{\mathrm{AA}}$, and $\varepsilon_{\mathrm{BB}}$ occur between the different pairs of monomers, the partition function is (assuming $\varepsilon_{\mathrm{AA}} = \varepsilon_{\mathrm{BB}}$ for simplicity)

$$Z = \sum q^{m_{\mathrm{AA}}+m_{\mathrm{BB}}} q_{\mathrm{AB}}^{m_{\mathrm{AB}}}, \quad q = \exp(-\varepsilon_{\mathrm{AA}}/k_{\mathrm{B}}T), \quad q_{\mathrm{AB}} = \exp(-\varepsilon_{\mathrm{AB}}/k_{\mathrm{B}}T) \quad (16)$$

where the sum is extended over all bottle brush configurations which are compatible with the excluded volume constraints, and m_{AA}, m_{BB}, and m_{AB} denote the numbers of nonbonded occupied nearest-neighbor monomers pairs AA, BB, and AB, respectively. Noting that for single chains the Theta-point in this model exists and occurs for[35] $q_\Theta = 1.3087$, the choice $q = 1.5$ was made to realize a bottle-brush polymer in the poor solvent regime.

Contrary to the theoretical predictions,[123,124] no long-range order of this Janus cylinder phase separation type was detected for this model. Defining a correlation function which measures the Janus cylinder-type short-range order along the cylinder axis, a corresponding correlation length ξ could be extracted.[43–45] However, it was found that this correlation length increases only rather slowly with increasing incompatibility $\varepsilon_{\mathrm{AB}} - (\varepsilon_{\mathrm{AA}} + \varepsilon_{\mathrm{BB}})/2$ while it increases roughly linear with the side chain length N (Figure 8). This failure to see any onset of long-range order (where ξ would diverge) is expected on general grounds, of course, since for finite side chain length N the bottle brush is a quasi-one-dimensional system, and general theorems forbid

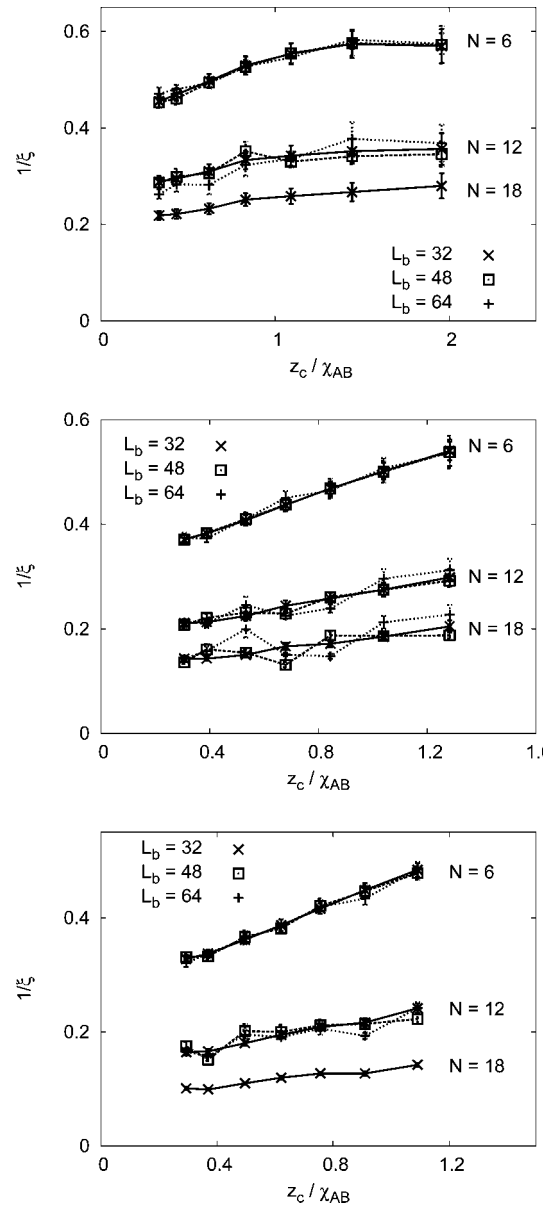

Figure 8. Plot of the inverse correlation length $1/\xi$ that measures Janus cylinder-type concentration correlations vs the inverse Flory−Huggins parameter z_c/χ_{AB}, for good solvent conditions ($q = 1$, case a), Theta-solvent conditions ($q = 1.3087$, case b), and poor solvent conditions ($q = 1.5$, case c). Data for three side chain lengths $N = 6$, 12, and 18 and three backbone lengths $L_{\mathrm{B}} = 32$, 48, and 64 are included as well. All data refer to the choice of one grafted polymer per grafting site. Reproduced with permission from ref 45. Copyright 2007 Wiley-VCH.

long-range order in one-dimensional systems with short-range forces.[125]

While for this model PERM is useful since a range of values for the side chain length N results from a single simulation, for small q_{AB} (and/or small q) the accuracy of the method deteriorates due to still too large fluctuations in the magnitudes of the weights. Also in this case the free energy was not the primary aim of the study, and thus PERM was not much superior to a standard type of Monte Carlo simulation (as done in ref 124). Nevertheless, rather definitive new results on the lack of Janus cylinder type phase separation were obtained, paying appropriate attention to the adequate analysis of the simulation data.

Speeding Up Dynamic Monte Carlo Algorithms by Special Moves: The Case of Polymer Melts

The Problem and Its Solution. Many problems of interest in polymer science concern dense melts where many long chains are randomly entangled with each other: phase separation in polymer blends,[126] mesophase ordering in block copolmyer melts,[126–128] liquid crystalline ordering in melts of semiflexible polymers,[129–131] etc. As a relatively efficient lattice model to deal with such problems, the bond fluctuation model was proposed about 20 years ago.[28–30] As far as dynamic Monte Carlo algorithms are concerned, it is distinguished e.g. from the simple self-avoiding walk model[8,49] in that a single type of Monte Carlo move suffices in practice to provide good equilibration, namely the "random hopping" move: a monomer is chosen at random and a direction in one of the six axes of the simple cubic lattice is chosen at random, and one attempts to move the monomer by one lattice unit in the chosen direction. This move is only carried out when it satisfies excluded volume and bond length constraints and when it passes the standard Metropolis[47–49,53] acceptance test, eq 8. A further advantage of this algorithm is that it yields a reasonable description of the chain dynamics in polymer melts,[2,21,22] compatible with the Rouse model[21] for short chains and crossing over to a behavior compatible with the reptation model[2,21] for long chains.[30,132]

However, if one is interested in static equilibrium properties only, the slow dynamics of long chains (according to reptation theory[2,21] the chain relaxation time of entangled chains increases according to a power law $\tau \propto N^3$) hampers efficient equilibration of the system.[31] Thus, it has been a widely used practice to randomly mix the above reptation move with a move according to the "slithering snake" (SS) algorithm.[31,49] In this algorithm, one randomly chooses an end monomer of the chain, and the trial move consists in detaching it and attempting to attach it to the opposite chain end (again excluded volume and bond length constraints are respected, and the Metropolis test needs to be passed[47–49,53]). While in the random hopping algorithm the chosen monomer moves only one lattice unit in a single step, the SS algorithm moves it of the order of the end-to-end distance, which is of order $\sqrt{N}$ lattice units.

Therefore, the chain diffusion constant is a factor of N larger than for the random hopping algorithm (where it scales as $D_N \propto 1/N$ for short chains[132]), and correspondingly the SS algorithm yields a relaxation time scaling $\tau \propto N^2$.[31,132] Thus, by random mixing in of these SS moves, it has been possible to study the Ising to mean-field crossover in the critical behavior of phase separation in symmetric polymer blends,[126,133] studying chain lengths from $N = 16$ to $N = 512$, and correlation hole effects in the structure of semidilute polymer solutions could even be studied for chains as long as $N = 2000$.[134] We are not aware of similar progress for block copolymer melt studies[126] or Monte Carlo studies of liquid crystalline order in melts of semiflexible chains,[129–131] however.

Wittmer et al.[27] recently succeeded to equilibrate dense melts of polymer chains described by the bond fluctuation model (melt behavior is already realized when a fraction $\phi = 0.5$ of lattice sites is occupied by corners of the effective monomers, which take each a whole elementary cube of the simple cubic lattice) for substantially larger chain lengths, namely up to $N = 8192$, choosing cubic simulation boxes of linear dimension $L = 256$ (with periodic boundary conditions), containing $2^{20} \approx 10^6$ effective monomers. This progress is due to implementation of two ideas: the first idea is to modify the local moves. Rather than choosing as a new position of the effective monomer only one out of the six positions when a nearest-neighbor distance is chosen (what we henceforth call L06 move), one chooses out of 26 positions of the cube surrounding the current monomer position (called L26 move). This move allows the chains to cross each other and hence no longer provides a realistic description of chain dynamics, where the fact is important that chains cannot cross in the course of their random motions, leading to reptation behavior.[2,21] However, being interested in equilibrium properties, such a chain crossing algorithm is perfectly legitimate to sample configuration space, since it satisfies the detailed balance principle, eq 5. If only such local moves L26 are considered, the dynamics is perfectly consistent with the Rouse model, one finds $\tau \approx 530N^2$ (Figure 9) while the L06 algorithm shows the Rouse model to reptation crossover.[30,135] Including also SS moves reduces the relaxation time further by about 1 order of magnitude, $\tau \approx 40N^2$ (Figure 9). As

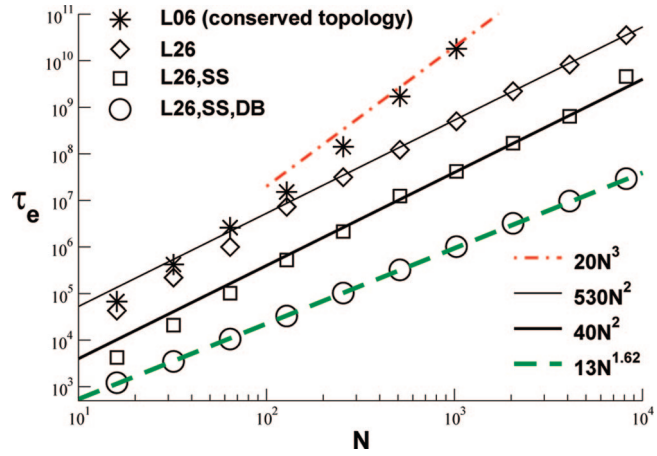

Figure 9. Diffusion time τ_e over the (root mean squared) chain end-to-end distance R_e on a log−log plot vs chain length, comparing different algorithms of the bond fluctuation model at a volume fraction $\phi = 0.5$. Asteriks denote the L06 algorithm that conserves the topology of the chains during their motions, diamonds the L26 algorithm that allows chain intersections, while squares refer to an algorithm where L26 and SS moves are mixed. If one allows in addition double-bridging moves (DB), the power law exponent changes from the Rouse value (2) to an empirical value 1.62. Straight lines show corresponding power law fits, as indicated. Reproduced with permission from ref 27. Copyright 2007 American Institute of Physics.

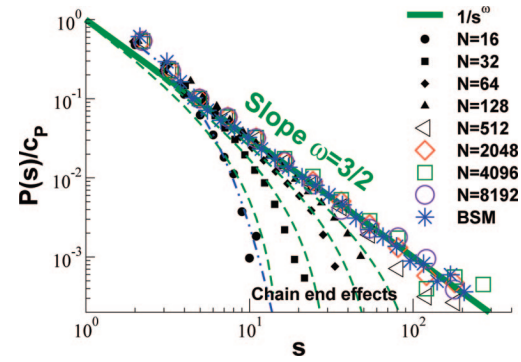

Figure 10. Bond−bond correlation function $P(s)/c_p$, where c_p is a constant allowing the comparison of different models,[27] on a log−log plot vs the curvilinear distance s. Various chain lengths are included, as indicated, and data for a bead−spring model (BSM) in the continuum with $N = 1024$ are included as well. The thick line shows the power law $1/s^{\omega}$ with slope $\omega = 3/2$. This power law is found to hold in the regime $1 \ll s \ll N$. The dash-dotted curve $P(s) \propto \exp(-s/1.5)$ shows that the exponential behavior of Gaussian chains is only compatible with the data for very short chains. The broken curves show a theoretical prediction that corrects the power law for chain-end effects. Reproduced with permission from ref 27. Copyright 2007 American Institute of Physics.

a note of warning, we mention that using SS moves only in a dense melt is inefficient, the strong "backjump correlation" leads to an exponential increase of τ with N,[136] and some numerical evidence for this prediction have indeed been observed.[137] It is also worth mentioning that for the algorithm L26 SS most of the CPU time is still used by the local moves.

A spectacular further improvement is possible by including "double-bridging" (DB) moves, which were originally suggested for equilibrating off-lattice models of polymer melts by Monte Carlo methods.[138–142] This type of connectivity altering move has the advantage of conserving monodispersity of the melt over earlier such connectivity-altering algorithms.[143,144] In the double-bridging algorithm an inner monomer of a chain attacks an inner monomer of another chain (or the same chain) and tries to form a trimer bridge. Simultaneously another bridge is formed between two monomers which are four steps apart from the first two monomers along the two chains, generating two new chains with exactly the same length as the original one. As for the SS moves, one uses all 108 bond vectors that the bond fluctuation model offers for the above-described switch of chain segments between two different chains (or the same chain). Note that chain intersections are again occurring here, which does not matter since we are concerned with equilibrium properties only. However, it is crucial to make sure that the implementation satisfies detailed balance, eq 5. This question arises since more than one swap partner is possible for a selected first monomer. To avoid this problem, all moves are refused which would be possible with more than one swap partner (this needs to be checked both for the move and the reverse move). To avoid immediate reverse moves, the frequency at which these DB moves are thrown in needs to be fairly low. But as Figure 9 shows, for $N = 1024$ the relaxation is faster by about 4 orders of magnitude in comparison with the L06 algorithm and about 2 orders of magnitude in comparison with the L26, SS algorithm; for $N = 8192$ this speed-up has further increased due to the smaller value of the exponent of N in the relation for the relaxation time.

Application: A Study of Intramolecular Long-Range Correlations in Melts. Here we return to the problem mentioned already in the Introduction, the announced deviations from the Flory ideality hypothesis[1,2,18–20] in dense melts of long chains. If it were true that intrachain interactions were perfectly canceled by interchain interactions so that the chain configurations strictly correspond to those of ideal random walks following the Gaussian chain statistics, one would conclude that any correlation function that one can consider will decay exponentially with distance s along the chain. Figure 10 shows that this expectation completely fails for the bond−bond correlation function of the chain[27]

$$P(s) = \langle \vec{l}_{n+s} \cdot \vec{l}_n \rangle / \langle \vec{l}_n^{\,2} \rangle, \quad \vec{l}_i \equiv \vec{r}_{i+1} - \vec{r}_i \tag{17}$$

where the averages $\langle \cdots \rangle$ include an average over all possible pairs of bonds along the chain ($\vec{r}_i$ is the site of the ith monomer) and over all chains.

Unfortunately, the bond−bond correlation defined in eq 17 cannot be measured via standard scattering experiments. For the standard intramolecular pair distribution function, which is experimentally accessible when one studies the small-angle scattering from melts via neutron scattering, when the melt contains a small fraction of deuterated chains while the majority of chains is protonated,[22] the long-range correlations lead only to a correction to the well-known Debye function[22] that should be visible when one performs a "Kratky plot".[22] That is, according to the Gaussian chain statistics, the structure factor $S(q)$ in the regime $1/\langle R_g^2 \rangle \ll q^2 \ll 1/\langle l^2 \rangle$ should be described by the relation $S(q) = S_0(q) = 12/(b^2 q^2)$, where b is the size of an "effective segment". So, a plot of $q^2 S(q)$ vs q in this regime should be constant ("Kratky plot"[22]). Because of the long-range correlations, one rather predicts a different behavior:[26]

$$S(q) = S_0(q)\left(1 - \frac{3}{8}\frac{q}{b^2 \rho}\right) \tag{18}$$

ρ being the monomer density in the system. However, since also nonuniversal corrections (due to chain stiffness, for instance) come in as well, when the condition $q^2 \ll 1/\langle l^2 \rangle$ is not strictly fulfilled, the clear experimental verification of eq 18 as yet is still lacking. We maintain, however, that the discovery of long-range correlations in polymer melts is an important facet in our theoretical understanding of polymers and possibly has far-reaching consequences. For example, a standard mean-field treatment of collective phenomena in two- or multicomponent dense polymer melts is the well-known "random phase approximation" (RPA),[2] where the collective structure factor of the system is expressed in terms of single-chain structure factors of the components contained in the melt. Since the RPA describes the single chain structure factor by the Debye function, which is not as accurate a description as has been assumed in the past, it is clear that the results discussed above also raise important questions on the accuracy of the RPA, even for the case of very long polymer chains. Also, many descriptions based on the simple "blob picture",[2] which asserts that excluded volume effects are only important inside of a blob while on larger scales the statistics of a chain in a semidilute or dense polymer solution is strictly Gaussian, may require reconsideration.

Formation of Micelles in Homopolymer−Copolymer Mixtures

When one deals with systems containing several types of monomers (A, B), such as polymer blends, block copolymers, etc., additional "unphysical" moves are a great advantage to equilibrate the system. For example, for symmetrical polymer blends an algorithm was devised[31,126,145,146] where A−B interchanges of whole polymer chains (not at all changing their configuration) were implemented. For an experimentalist, such an "identity switch" of a chain may sound like alchemy; for a theorist, this move simply implements a different ensemble of statistical mechanics, namely the "semi-grand canonical ensemble" of the mixture, where the chemical potential difference $\Delta\mu$ rather than the composition of the mixture is the independently given control parameter. Although this control parameter normally is not available in the laboratory, statistical mechanics tells us that the different ensembles of statistical mechanics are fully equivalent to each other in the thermodynamic limit. Combining the simulation in the $(\Delta\mu VT)$ ensemble (V is the volume of the simulation box), then with a finite size scaling analysis[145,146] which provides an extrapolation to the thermodynamic limit, $V \to \infty$, valid results which are also significant for the interpretation of experiments were obtained.[126,133] A drawback of this approach, namely the requirement of a strict symmetry with respect to the chain lengths, $N_A = N_B$, was later alleviated by an algorithm that only requires $N_A = kN_B$, with $k = 2, 3, 4, \ldots$, where an A chain is cut into k equally long pieces which turn into B, or vice versa (k B chains need to be connected and turned into A).[147,148]

We describe here in detail only the simplest case, namely a symmetrical polymer blend. In the grand canonical ensemble the independent control parameters would be the chemical potentials μ_A and μ_B of A monomers and B monomers. For chain lengths $N_A = N_B = N$ the partition function Z_G then is

$$Z_G = \sum_{\text{conf}} \exp\left\{\frac{\mu_A n_A N + \mu_B n_B N}{k_B T}\right\} \exp\left\{-\frac{E(\text{conf})}{k_B T}\right\} \quad (19)$$

where n_A (n_B) are the numbers of A (B) chains in the considered configuration, and the energy E(conf) contains all the interaction energies between the different monomers which we assume to be pairwise. In the semi-grand canonical ensemble $n = n_A + n_B$ is fixed, and then it is useful to introduce as an order parameter the relative difference m in the number of chains, $m = (n_A - n_B)/(n_A + n_B)$. Introducing $\Delta\mu = \mu_A - \mu_B$ the first exponential in eq 20 can be rewritten as

$$\exp\left\{\frac{\mu_A n_A N + \mu_B n_B N}{k_B T}\right\} = \exp\left\{\frac{nN(\mu_A + \mu_B)}{2k_B T}\right\} \exp\left\{\frac{nNm\Delta\mu}{2k_B T}\right\} \quad (20)$$

An identity switch A→ B or vice versa of a chain at fixed conformation is then controlled by the following transition probability

$$W(c \rightarrow c') = \min\left\{1, \exp\left[\frac{Nn\Delta\mu(m' - m)}{2k_B T}\right] \times \exp\left[-\frac{E(c') - E(c)}{2k_B T}\right]\right\} \quad (21)$$

Of course, the identity switch will change the order parameter m to m' and the chemical potential difference $\Delta\mu$ controls the correspondig part of the acceptance rate of the move. The other part is determined by the energy change $\Delta E = E(c') - E(c)$ caused by the change in the numbers of AA, AB, and BB pairs. Near the critical point of a binary polymer blend the typcial energy change $|\Delta E/k_B T|$ is of order unity, and thus eq 21 leads to reasonably large acceptance probabilities.

A variation on the theme was recently implemented for mixtures of homopolymers of type B (chain length $N_B = N$) and (asymmetric) block copolymers of the same chain length N and composition f {length of the A block being $N_A = fN$, length of the B block $N_B = (1 - f)N$},[46] with $f = 1/8$. The range of chain lengths was from $N = 48$ to $N = 128$ only; thus, it was sufficient to mix the L06 and SS algorithms to relax the chain configurations, and a cubic simulation box with a linear dimension of $L = 96$ lattice spacings was used. The "most symmetric" nontrivial choice of interactions was taken, $\varepsilon_{AB} = -\varepsilon_{AA} = -\varepsilon_{BB} = \varepsilon$, of a square-well form extended over the nearest 54 lattice sites as in the polymer blend studies.[146–148] This study then also applies a semi-grand canonical ensemble, but $\Delta\mu$ now is the chemical potential difference not between A and B, but between a block copolymer of the chosen composition and a homopolymer. So the total number of chains in the system, $\mathbf{N} = \mathbf{N}_{A_f B_{1-f}} + \mathbf{N}_B$, is held fixed, but the fraction of copolymers is allowed to fluctuate. In this way, it has been possible to study micellization for rather large chain lengths and aggregate sizes (containing up to 10^4 monomers) in full thermal equilibrium, i.e., without constraining the number of block copolymers forming a micelle. This would not have been feasible working in the canonical ensemble, where micelles have extremely large relaxation times and are notoriously hard to equilibrate.

Being interested in a test of theoretical descriptions based on the self-consistent-field (SCF) theory,[127,128] we work at rather large incompatibility between A and B, namely choosing $\varepsilon N = 19.2$.

Typical results for the number size distribution $P(n_{AB})$ of the number of chains inside a micelle, at a state slightly above the critical micelle concentration, are shown in Figure 11. Since the self-consistent-field theory predicts that the number n_{AB} of block copolymers in a micelle at fixed χN (χ being the Flory−Huggins parameter[1]) should scale like $n_{AB} \propto \sqrt{N}$, and a fixed value of εN should correspond to a fixed value of χN, we

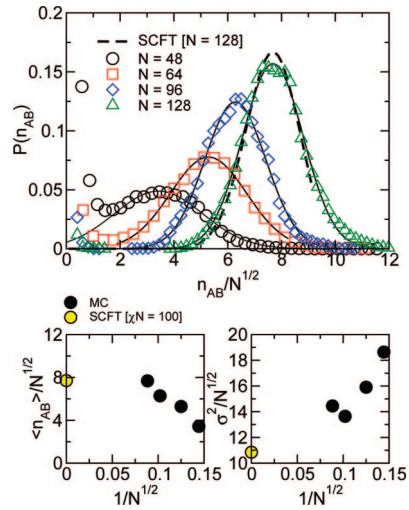

Figure 11. Upper panel: the micelle number size distribution $P(n_{AB})$ as a function of the scaled aggregation number $n_{AB}/\sqrt{N}$. The symbols show the simulation data, the thick lines a fit with a Gaussian function. For the largest chain length, $N = 128$, the SCF results for $\chi N = 100$ (which should correspond to the chosen value of εN) and $\delta\mu_{coex} = 6.0$ are also shown as dashed line. The normalization of the SCF result was chosen such that the weight of the right peak (micelles) equals the result of the Monte Carlo simulations. Lower panels: the scaled average aggregation number $\langle n_{AB}\rangle/\sqrt{N}$ and the scaled standard deviation $\sigma^2/\sqrt{N}$ are plotted vs $1/\sqrt{N}$. The latter data (full dots) are obtained from the Gaussian fits in the upper panel. Open circles at the ordinate axis are the SCF predictions for $\chi N = 100$. Reproduced with permission from ref 46. Copyright 2006 American Chemical Society.

plot $P(n_{AB})$ as a function of $n_{AB}\sqrt{N}$ due to the expectation from SCF theory to see date collapse. While the size of the micelles is found to be Gaussianly distributed around the mean value $\langle n_{AB}\rangle$, as SCF theory also predicts, one does not observe the expected scaling behavior: instead of a data collapse, one only observes a very gradual approach to the asymptotic behavior. In the region studied, the growth of the micelle size with chain length is stronger than predicted by the SCF theory. When one tries an extrapolation of the scaled position $\langle n_{AB}\rangle/N^{1/2}$ and scaled width $\sigma^2/N^{1/2}$ of the distribution versus $N^{-1/2}$, the latter seems compatible with the expectation that SCF theory becomes correct in the limit $N \rightarrow \infty$, while with respect to $\langle n_{AB}\rangle/N^{1/2}$ no such conclusion can be drawn.

When one studies geometrical properties of the micelles, similar (though somewhat less pronounced) deviations from scaling are encountered, and the approach toward the SCF limit is always rather slow. Cavallo et al.[46] mention several reasons for this problem with SCF theory: (i) For all values of N the chain length of the A block, $N_A = fN = N/8$, is fairly short, so excluded volume effects are not yet fully screened out and give rise to systematic deviations. (ii) In the mapping between the energy scale ε of the simulated model and the Flory−Huggins parameter χ also a correction of order $1\sqrt{N}$ is needed. (iii) The size of the AB interface is broadened compared to the SCF prediction. These deviations stem from shape fluctuations of the micelle, which are ignored within the mean-field approximation that underlies SCF theory.

Even though all these reasons why deviations from SCF theory should be expected are perfectly reasonable, we emphasize that in practical applications the limit $N \rightarrow \infty$ for micelle formation is hardly relevant; considering that one effective monomer of the bond fluctuation model may correspond to several chemical monomers, we note that the range of N studied in Figure 8 coincides with the range of experimental interest.

Thus, quantitative fits of experimental data to SCF theory need to be taken with great precautions.

Discussion and Outlook

In this paper we have not attempted to give a comprehensive review of all the important current trends in the Monte Carlo simulation of polymers, but rather gave a selection of problems dealing with lattice models of polymers, where due to advances in simulation methodology (such as the Wang−Landau and PERM algorithms and the combination of chain-intersecting moves and double-bridging moves in the bond fluctuation model) significant progress with rather basic problems of theoretical polymer physics could be achieved. Of course, this selection of problems and techniques is strongly biased by the interests of the authors and their expertise; this has been the main reason for the focus on work from their own research group. In fact, very interesting applications of the Wang−Landau and PERM algorithms (as well as their extensions such as FLATPERM[69] and related advanced techniques such as multicanonical sampling[149,150]) exist for closely related problems[151–153] also including the well-known HP-lattice model for protein folding.[154–156] We do expect that much important work will be forthcoming along such lines.

A completely different but certainly no less important direction concerns the application of advanced off-lattice Monte Carlo methods to study problems such as the structure of interfaces between a crystalline substrate and amorphous regions of polymers (applying algorithms involving double-bridging and other sophisticated nonlocal moves for chemically realistic atomistic models[157]), development of coarse-grained models for the description of the equation of state of polymer solutions,[158] and the development of coarse-graining strategies for dense polymer melts.[159] A very interesting approach, applicable for semidilute polymer solutions[160] and polymer brushes[161] involves a coarse-graining where a (soft) particle does not correspond just only to a small number of successive monomers along a chain, but represents a whole "blob". Such models are intermediate between the standard models for polymers, as treated here, and very crude models where a whole polymer coil is represented by one soft particle.[162] Such models have been suggested for the description of polymer blends,[162] but also the Asakura−Oosawa model of colloid−polymer mixtures[163,164] is an extreme variant of this class of models (polymers are described as spheres whose mutual overlap does not cost any energy; only their overlap with the colloidal particles is forbidden).

In conclusion, we can say that the field of Monte Carlo simulation of polymers is rapidly progressing and has matured to a stage where it can make both a large impact to problems in basic theoretical polymer physics (as described here) and materials science-type problems, involving polymers (not described here). A large body of know-how about simulation techniques has been accumulated in the literature.[165,166] While we clearly could not give details about these techniques in our paper, we hope it will serve as a useful guide to the literature. Last but not least, it should help the practitioner to think about the difficult question "when should which algorithm be applied?", since it is often decisive for making progress to adapt the model and the algorithm with which it is simulated to the problem at hand.

Acknowledgment. We are grateful to A. P. Cavallo, H.-P. Hsu, J. Luettmer-Strathmann, M. Müller, F. Rampf, and T. Strauch for a fruitful collaboration about research projects leading to some of the results described in this paper. We are particularly indebted to J. Bachnagel and J. Wittmer for allowing us to include some results taken from their work (Figures 9 and 10 are taken from ref 27). This research is supported in part by the Deutsche Forschungsgemeinschaft, SFB 625/A3.

References and Notes

(1) Flory, P. J. *Principles of Polymer Chemistry*; Cornell University Press: Ithaca, NY, 1953.
(2) de Gennes, P. G. *Scaling Concepts in Polymer Physics*; Cornell Universtiy Press: Ithaca, NY, 1979.
(3) des Cloizeaux, J.; Jannink, G. *Polymers in Solution: Their Modelling and Structure*; Clarendon Press: Oxford, 1990.
(4) Grosberg, A. Yu.; Khokhlov, A. R. *Statistical Physics of Macromolecules*; AIP Press: New York, 1994.
(5) Schäfer, L. *Excluded Volume Effects in Polymer Solutions*; Springer: Berlin, 1999.
(6) Rubinstein, M.; Colby, R. H. *Polymer Physics*; Oxford University Press: Oxford, 2003.
(7) Le Guillou, J. C.; Zinn-Justin, J. *Phys. Rev. B* **1980**, *21*, 3976–98.
(8) Sokal, A. D. In *Monte Carlo and Molecular Dynamics Simulations in Polymer Science*; Binder, K., Ed.; Oxford University Press: New York, 1995.
(9) Prellberg, T. *J. Phys. A: Math. Gen.* **2001**, *34*, L599−602.
(10) Nienhuis, B. *Phys. Rev. Lett.* **1982**, *49*, 1062–1065.
(11) Duplantier, B. *J. Phys. (Paris)* **1982**, *43*, 991–1019.
(12) Duplantier, B. *J. Chem. Phys.* **1987**, *86*, 4233–4244.
(13) Lifshitz, I. M.; Grosberg, A. Y.; Khokhlov, A. R. *Rev. Mod. Phys.* **1978**, *50*, 683–713.
(14) Rampf, F.; Paul, W.; Binder, K. *Europhys. Lett.* **2005**, *70*, 628–634.
(15) Rampf, F.; Paul, W.; Binder, K. *J. Polym. Sci., Part B: Polym. Phys.* **2006**, *44*, 2542–2555.
(16) Paul, W.; Rampf, F.; Strauch, T.; Binder, K. *Macromol. Symp.* **2007**, *252*, 1–11.
(17) Paul, W.; Strauch, T.; Rampf, F.; Binder, K. *Phys. Rev. E* **2007**, *75*, 060201.
(18) Flory, P. J. *J. Chem. Phys.* **1945**, *17*, 453–65.
(19) Flory, P. J. *J. Chem. Phys.* **1949**, *17*, 303–16.
(20) Flory, P. J. *Statistical Mechanics of Chain Molecules*; Oxford University Press: New York, 1988.
(21) Doi, M.; Edwards, S. F. *The Theory of Polymer Dynamics*; Clarendon Press: Oxford, 1986.
(22) Strobl, G. R. *The Physics of Polymers. Concepts for Understanding Their Structure and Behavior*; Springer: Berlin, 1997.
(23) Semenov, A. N.; Johner, A. *Eur. Phys. J. E* **2003**, *12*, 469–80.
(24) Semenov, A. N.; Obukhov, S. P. *J. Phys.: Condens. Matter* **2005**, *17*, 1747–62.
(25) Wittmer, J. P.; Meyer, H.; Baschnagel, J.; Johner, A.; Obukhov, S. P.; Mattioni, L.; Müller, M.; Semenov, A. N. *Phys. Rev. Lett.* **2004**, *93*, 147801.
(26) Wittmer, J. P.; Beckrich, P.; Johner, A.; Semenov, A. N.; Obukhov, S. P.; Meyer, H.; Baschnagel, J. *Europhys. Lett.* **2007**, *77*, 56003.
(27) Wittmer, J. P.; Beckrich, P.; Meyer, H.; Cavallo, A.; Johner, A.; Baschnagel, J. *Phys. Rev. E* **2007**, *76*, 011803.
(28) Carmesin, I.; Kremer, K. *Macromolecules* **1988**, *21*, 2819–23.
(29) Deutsch, H.-P.; Binder, K. *J. Chem. Phys.* **1991**, *94*, 2294–2904.
(30) Paul, W.; Binder, K.; Heermann, D.; Kremer, K. *J. Phys. II* **1991**, *1*, 37–60.
(31) Binder, K. In *Monte Carlo and Molecular Dynamics Simuations in Polymer Science*; Binder, K., Ed.; Oxford University Press: New York, 1995.
(32) Wang, F.; Landau, D. P. *Phys. Rev. Lett.* **2001**, *86*, 2050–2053.
(33) Wang, F.; Landau, D. P. *Phys. Rev. E* **2001**, *64*, 056101.
(34) Luettmer-Strathmann, J.; Paul, W.; Rampf, F.; Binder, K. *J. Chem. Phys.* **2008**, *128*, 064903.
(35) Grassberger, P. *Phys. Rev. E* **1997**, *56*, 3682–93.
(36) Hsu, H. P.; Mehra, V.; Nadler, W.; Grassberger, P. *Phys. Rev. E* **2003**, *68*, 1–4.
(37) Hsu, H.-P.; Grassberger, P. *Europhys. Lett.* **2004**, *66*, 874–80.
(38) Hsu, H.-P.; Nadler, W.; Grassberger, P. *Macromolecules* **2004**, *37*, 4658–63.
(39) Hsu, H.-P.; Nadler, W.; Grassberger, P. *J. Phys. A: Math. Gen.* **2005**, *38*, 775–806.
(40) Rosenbluth, M. N.; Rosenbluth, A. W. *J. Chem. Phys.* **1955**, *23*, 356–59.
(41) Hsu, H.-P.; Grassberger, P. *Eur. Phys. J. B* **2003**, *36*, 209–14.
(42) Hsu, H.-P.; Binder, K.; Klushin, L. I.; Skvortsov, A. M. *Phys. Rev. E* **2007**, *76*, 021108.
(43) Hsu, H.-P.; Paul, W.; Binder, K. *Europhys. Lett.* **2006**, *76*, 526–532.
(44) Hsu, H.-P.; Paul, W.; Binder, K. *Macromol. Symp.* **2007**, *252*, 58–67.
(45) Hsu, H.-P.; Paul, W.; Binder, K. *Macromol. Theory Simul.* **2007**, *16*, 660–689.

(46) Cavallo, A.; Müller, M.; Binder, K. *Macromolecules* **2006**, *39*, 9539–9950.
(47) Binder, K.; Heermann, D. W. *Monte Carlo Simulation in Statistical Physics. An Introduction*; Springer: Berlin, 1988.
(48) Landau, D. P.; Binder, K. *A Guide to Monte Carlo Simulations in Statistical Physics*, 2nd ed.; Cambridge University Press: Cambridge, 2005.
(49) Kremer, K.; Binder, K. *Comput. Phys. Rep.* **1988**, *7*, 259–310.
(50) Ohno, K.; Binder, K. *J. Stat. Phys.* **1991**, *64*, 781–806.
(51) Ohno, K.; Sakamoto, T.; Minagawa, T.; Okabe, Y. *Macromolecules* **2007**, *40*, 723–30.
(52) Eisenriegler, E.; Kremer, K.; Binder, K. *J. Chem. Phys.* **1982**, *77*, 6296–6320.
(53) Metropolis, N.; Rosenbluth, A. W.; Rosenbluth, M. N.; Teller, A. H.; Teller, E. *J. Chem. Phys.* **1953**, *21*, 1087–92.
(54) Shell, M. S.; Debenedetti, P. G.; Panagiotopoulos, A. Z. *Phys. Rev. E* **2002**, *66*, 056703.
(55) Yan, Q. L.; Faller, R.; de Pablo, J. J. *J. Chem. Phys.* **2002**, *116*, 8745–8749.
(56) Yan, Q. L.; de Pablo, J. J. *Phys. Rev. Lett.* **2003**, *90*, 035701.
(57) Yan, Q. L.; Jain, T. S.; de Pablo, J. J. *Phys. Rev. Lett.* **2004**, *92*, 235701.
(58) Mastny, E. A.; de Pablo, J. J. *J. Chem. Phys.* **2005**, *122*, 124109.
(59) Rathore, N.; de Pablo, J. J. *J. Chem. Phys.* **2002**, *116*, 7225–7230.
(60) Rathore, N.; Knotts, T. A.; de Pablo, J. J. *J. Chem. Phys.* **2003**, *118*, 4285−4290, 9460−9461.
(61) Rathore, N.; Knotts, T. A.; de Pablo, J. J. *Biophys. J.* **2003**, *85*, 3963–3968.
(62) Belardinelli, R. E.; Pereyra, V. D. *Phys. Rev. E* **2007**, *75*, 046701.
(63) Schulz, B. J.; Binder, K.; Müller, M. *Int. J. Mod. Phys.* **2002**, *13*, 477–494.
(64) Trebst, S.; Huse, D. A.; Troyer, M. *Phys. Rev. E* **2004**, *70*, 046701.
(65) Shell, M. S.; Debenedetti, P. G.; Panagiotopoulos, A. Z. *J. Chem. Phys.* **2003**, *119*, 9406–9411.
(66) Zhang, C.; Ma, J. *Phys. Rev. E* **2007**, *76*, 036708.
(67) Chopra, M.; Müller, M.; de Pablo, J. J. *J. Chem. Phys.* **2006**, *124*, 134102.
(68) Müller, M.; de Pablo, J. J. In *Computer Simulations in Condensed Matter: From Materials to Chemical Biology*; Ferrario, M., Ciccotti, G., Binder, K., Eds.; Springer: Heidelberg, 2006; Vol. *1*, pp 67−126.
(69) Prellberg, T.; Krawczyk, J. *Phys. Rev. Lett.* **2004**, *92*, 120602.
(70) Paul, W.; Müller, M. *J. Chem. Phys.* **2001**, *115*, 630–635.
(71) Sommer, J.-U., Reiter, G., Eds. *Polymer Crystallization: Observation, Concepts, and Interpretation*; Springer: Berlin, 2003.
(72) Binder, K.; Baschnagel, J.; Müller, M.; Paul, W.; Rampf, F. *Macromol. Symp.* **2006**, *237*, 128–138.
(73) Binder, K.; Baschnagel, J.; Paul, W. *Prog. Polym. Sci.* **2003**, *28*, 115–172.
(74) Binder, K.; Kob, W. *Glassy Materials and Disordered Solids. An Introduction to Their Statistical Mechanics*; World Scientific: Singapore, 2005.
(75) Lekkerkerker, H. N. W.; Poon, W. K. C.; Pusey, P. N.; Stroobants, A.; Warren, P. B. *Europhys. Lett.* **1990**, *20*, 559–564.
(76) Ilett, S. M.; Orrock, A.; Poon, W. K. C.; Pusey, P. N. *Phys. Rev. E* **1995**, *51*, 1344–1352.
(77) Noro, M. G.; Frenkel, D. *J. Chem. Phys.* **2000**, *113*, 2941–2944.
(78) Khokhlov, A. R. *Polym. Sci. U.S.S.R.* **1979**, *21*, 2185–95.
(79) Grosberg, A.Yu.; Khokhlov, A. R. *Adv. Polym. Sci.* **1981**, *41*, 53–97.
(80) Khokhlov, A. R.; Semenov, A. N. *J. Stat. Phys.* **1985**, *38*, 161–182.
(81) Khokhlov, A. R.; Semenov, A. N. *Macromolecules* **1986**, *19*, 373–78.
(82) Ivanov, V. A.; Paul, W.; Binder, K. *J. Chem. Phys.* **1998**, *109*, 5659–5669.
(83) Stukan, M. R.; Ivanov, V. A.; Grosberg, A. Y.; Paul, W.; Binder, K. *J. Chem. Phys.* **2003**, *108*, 3392–3400.
(84) Martemyanova, J. A.; Stukan, M. R.; Ivanov, V. A.; Müller, M.; Paul, W.; Binder, K. *J. Chem. Phys.* **2005**, *122* (174907), 1–10.
(85) Wilding, N. B.; Müller, M.; Binder, K. *J. Chem. Phys.* **1996**, *105*, 802–909.
(86) Vrbová, T.; Whittington, S. G. *J. Phys. A: Math. Gen.* **1996**, *29*, 6253–6254.
(87) Vrbová, T.; Whittington, S. G. *J. Phys. A: Math. Gen.* **1998**, *31*, 3989–3998.
(88) Vrbová, T.; Procházka, K. *J. Phys. A: Math. Gen.* **1999**, *32*, 5469–5475.
(89) Singh, Y.; Giri, D.; Kumar, S. *J. Phys.: Math. Gen.* **2001**, *34*, L67−L74.
(90) Rajesh, R.; Dhar, D.; Giri, D.; Kumar, S.; Singh, Y. *Phys. Rev. E* **2002**, *65*, 056124.
(91) Misha, P.; Giri, D.; Kumar, S.; Singh, Y. *Physica A* **2003**, *318*, 737–772.
(92) Metzger, S.; Müller, M.; Binder, K.; Baschnagel, J. *J. Chem. Phys.* **2003**, *118*, 8489–8499.
(93) Krawczyk, J.; Owczarek, A. L.; Prellberg, T.; Rechnitzer, A. *Europhys. Lett.* **2005**, *70*, 726–732.
(94) Owczarek, A. L.; Rechnitzer, A.; Krawczyk, J.; Prellberg, T. *J. Phys. A: Math. Theor.* **2007**, *40*, 13257–13267.
(95) Vogel, T.; Bachmann, M.; Janke, W. *Phys. Rev. E* **2007**, *76*, 061803.
(96) de Gennes, P. G. *Macromolecules* **1980**, *13*, 1069–75.
(97) Rubin, R. S. *J. Chem. Phys.* **1965**, *43*, 2392–407.
(98) Eisenriegler, E. *Polymers Near Surfaces*; World Scientific: Singapore, 1993.
(99) Vanderzande, C. *Lattice Models of Polymers*; Cambridge University Press: Cambridge, 1998.
(100) Kreer, T.; Metzger, S.; Müller, M.; Binder, K.; Baschnagel, J. *J. Chem. Phys.* **2004**, *120*, 4012–4023.
(101) De Bell, K.; Lookman, T. *Rev. Mod. Phys.* **1993**, *65*, 87–113.
(102) Metzger, S.; Müller, M.; Binder, K.; Baschnagel, J. *Macromol. Theory Simul.* **2002**, *11*, 985–995.
(103) Subramanian, G.; Williams, D. R. M.; Pincus, P. A. *Europhys. Lett.* **1995**, *29*, 285–90.
(104) Subramanian, G.; William, D. R. M.; Pincus, P. A. *Macromolecules* **1996**, *29*, 4045–50.
(105) Jimenez, J.; Rajagopolan, R. *Langmuir* **1998**, *14*, 2598–601.
(106) Milchev, A.; Yamakov, V.; Binder, K. *Europhys. Lett.* **1999**, *47*, 675–680.
(107) Milchev, A.; Yamakov, V.; Binder, K. *Phys. Chem. Chem. Phys.* **1999**, *1*, 2083–2091.
(108) Sevick, E. M.; Williams, D. R. M. *Macromolecules* **1999**, *32*, 6841–46.
(109) Ennis, J.; Sevick, E. M.; Williams, D. R. M. *Phys. Rev. E* **1999**, *60*, 6906–18.
(110) Skvortsov, A. M.; Klushin, L. I.; Leermakers, F. A. M. *Europhys. Lett.* **2002**, *58*, 292–98.
(111) Klushin, L. I.; Skvortsov, A. M.; Leermakers, F. A. M. *Phys. Rev. E* **2004**, *69*, 061101.
(112) Skvortsov, A. M.; Klushin, L. I.; Leermakers, F. A. M. *J. Chem. Phys.* **2007**, *126*, 024905.
(113) Milchev, A.; Binder, K. *Eur. Phys. J. B* **1998**, *3*, 477–484.
(114) Hsu, H.-P.; Grassberger, P. *J. Chem. Phys.* **2004**, *120*, 2034–2041.
(115) Krawczyk, J.; Prellberg, T.; Owczarek, A. L.; Rechnitzer, A. *J. Stat. Mech. Theor. Exp.* **2004**, P 10004.
(116) Krawczyk, J.; Prellberg, T.; Owczarek, A. L.; Rechnitzer, A. *J. Stat. Mech. Theor. Exp.* **2005**, P 05008.
(117) Kahn, H. In *Symposium on the Monte Carlo Method*; Meyer, H. A., Ed.; Wiley: New York, 1956.
(118) Liu, J. S. *Monte Carlo Strategies in Scientific Computing*; Springer: Berlin, 2001.
(119) Reisner, W.; Morton, K. J.; Rühn, R.; Wang, Y. M.; Yu, Z.; Rosen, M.; Sturm, J. C.; Chou, S. Y.; Frey, E.; Austin, R. H. *Phys. Rev. Lett.* **2005**, *94*, 196101.
(120) Daoud, M.; de Gennes, P. G. *J. Phys. (Paris)* **1977**, *38*, 85–93.
(121) Stephan, T.; Muth, S.; Schmidt, M. *Macromolecules* **2002**, *35*, 9857–60.
(122) Li, C.; Gunari, K.; Janshoff, A.; Schmidt, M. *Angew. Chem., Int. Ed* **2004**, *43*, 1101–4.
(123) Stepanyan, R.; Subbotin, A.; ten Brinke, G. *Macromolecules* **2002**, *35*, 5640–8.
(124) de Jong, J.; ten Brinke, G. *Macromol. Theory Simul.* **2004**, *13*, 318–27.
(125) Domb, C., Green, M. S., Eds.; *Phase Transitions and Critical Phenomena*; Academic Press: New York, 1971; Vol. *1*.
(126) Binder, K. *Adv. Polym. Sci.* **1994**, *112*, 181–299.
(127) Hamley, I. W. *The Physics of Block Copolymers*; Oxford University Press: New York, 1998.
(128) Fredrickson, G. H. *The Equilibrium Theory of Inhomogenous Polymers*; Oxford University Press: New York, 2006.
(129) Weber, H.; Paul, W.; Binder, K. *Phys. Rev. E* **1999**, *59*, 2168–2174.
(130) Stukan, M. R.; Ivanov, V. A.; Müller, M.; Paul, W.; Binder, K. *J. Chem. Phys.* **2002**, *117*, 9934–9941.
(131) Ivanov, V. A.; An, E. A.; Spirin, L. A.; Stukan, M. R.; Müller, M.; Paul, W.; Binder, K. *Phys. Rev. E* **2007**, *76*, 016702.
(132) Binder, K.; Paul, W. *J. Polym. Sci., Part B: Polym. Phys.* **1997**, *35*, 1–31.
(133) Deutsch, H.-P.; Binder, K. *J. Phys. II* **1993**, *3*, 1049–1073.
(134) Schäfer, L.; Müller, M.; Binder, K. *Macromolecules* **2000**, *33*, 4568–4580.
(135) Kreer, T.; Baschnagel, J.; Müller, M.; Binder, K. *Macromolecules* **2001**, *34*, 1105–1117.
(136) Semenov, A. N. In *Theoretical Challenges in Dynamics of Complex Fluids*; McLeish, T., Ed.; Kluwer: Dordrecht, 1997.
(137) Mattioni, L.; Wittmer, J. P.; Baschnagel, J.; Barrat, J.-L.; Luijten, E. *Eur. Phys. J. E* **2003**, *10*, 369–85.

(138) Karayiannis, N.; Mavrantzas, V.; Theodorou, D. *Phys. Rev. Lett.* **2002**, *88*, 105503.
(139) Karayiannis, N.; Giannousaki, A.; Mavrantzas, V.; Theodorou, D. *J. Chem. Phys.* **2002**, *117*, 5465–79.
(140) Theordorou, D. N. In *Bridging Time Scales: Molecular Simulations for the Next Decade*; Nielaba, P., Mareschal, M., Ciccotti, G., Eds.; Springer: Berling, 2002.
(141) Mavrantzas, V. G. In *Handbook of Materials Modeling*; Yip, S., Ed.; Springer: Berlin, 2005; Vol. *I*.
(142) Banaszak, B. J.; de Pablo, J. J. *J. Chem. Phys.* **2003**, *119*, 2456–2462.
(143) Pant, P. V. K.; Theodorou, D. N. *Macromolecules* **1995**, *28*, 7224–7234.
(144) Uhlherr, A.; Mavrantzas, V. G.; Doxastakis, M.; Theodorou, D. N. *Macromolecules* **2001**, *34*, 8554–8568.
(145) Sariban, A.; Binder, K. *J. Chem. Phys.* **1987**, *86*, 5859–5873.
(146) Deutsch, H.-P.; Binder, K. *Macromolecules* **1992**, *25*, 6214–6230.
(147) Müller, M.; Binder, K. *Macromolecules* **1995**, *28*, 1825–1834.
(148) Müller, M. *Macromol. Theory Simul.* **1998**, *8*, 343–374.
(149) Berg, B. A.; Neuhaus, T. *Phys. Rev. Lett.* **2002**, *68*, 9–12.
(150) Berg, B. A. *J. Stat. Phys.* **1996**, *82*, 323–342.
(151) Bachmann, M.; Janke, W. *Phys. Rev. Lett.* **2005**, *95*, 058102.
(152) Bachmann, M.; Janke, W. *Phys. Rev. Lett.* **2003**, *91*, 208105.
(153) Bachmann, M.; Janke, W. *J. Chem. Phys.* **2004**, *120*, 6779–91.
(154) Dill, K. A. *Biochemistry* **1985**, *24*, 1501–9.
(155) Lau, K. F.; Dill, K. A. *Macromolecules* **1989**, *22*, 3986–97.
(156) Hsu, H.-P.; Mehra, V.; Nadler, W.; Grassberger, P. *J. Chem. Phys.* **2003**, *118*, 444–51.
(157) Daoulas, K.Ch.; Harmandaris, V. A.; Mavrantzas, V. G. *Macromolecules* **2005**, *38*, 5780–5795.
(158) Binder, K.; Müller, M.; Virnau, P.; MacDowell, L. G. *Adv. Polym. Sci.* **2005**, *173*, 1–110.
(159) Voth, G., Ed. *Coarse Graining of Condensed Phase and Biomolecular Systems*; Taylor and Francis: Boca Raton, FL, 2008 (in press).
(160) Krakoviack, V.; Hansen, J. P.; Louis, A. A. *Phys. Rev. E* **2003**, *67*, 041801.
(161) Coluzza I.; Hansen, J. P., preprint.
(162) Murat, M.; Kremer, K. *J. Chem. Phys.* **1998**, *708*, 4340–4348.
(163) Asakura, S.; Oosawa, F. *J. Chem. Phys.* **1954**, *22*, 1255–1256.
(164) Vink, R. L. C.; Horbach, J.; Binder, K. *Phys. Rev. E* **2005**, *71*, 011401.
(165) Kotelyanski, M. J., Theodorou, D. N., Eds. *Simulation Methods for Polymers*; Marcel Dekker: New York, 2004.
(166) Ferrario, M., Ciccotti, G., Binder, K., Eds. *Computer Simulations in Condensed Matter: From Materials to Chemical Biology*; Springer: Berlin, 2006; Vols. *1* and *2*.

MA702843Z